

# Hot Corrosion of Aluminized 1020 Steel with NaCl Deposit

*by* Sugiyanto Sugiyanto

---

**Submission date:** 06-Aug-2019 09:58AM (UTC+0800)

**Submission ID:** 1157958072

**File name:** 5.\_Sugiyanto,\_Journal\_International-Advanced\_Materials\_R..pdf (804.39K)

**Word count:** 2227

**Character count:** 11210

## Hot Corrosion of Aluminized 1020 Steel with NaCl Deposit

Mohammad Badaruddin<sup>1,a</sup>, Sugiyanto<sup>2,b</sup>

<sup>1,2</sup>Mechanical Engineering Department-University of Lampung

Jalan Prof. Brojonegoro No. 1 Bandar Lampung 35145, Indonesia

Tel: +62721-355519, Fax: +62721-704947

<sup>a</sup>mbruddin@unila.ac.id, <sup>b</sup>sugi@unila.ac.id

**Keywords:** AISI 1020 steel, aluminum coating, NaCl deposit, alumina scale, oxychlorination

**Abstract.** The oxidation of hot-dip aluminized AISI 1020 steel coated with NaCl in static air at 700 °C for a duration of time 49 h was studied by employing thermogravimetry, Scanning Electron Microscopy (SEM), Electron Dispersive Spectroscopy (EDS) and X-ray Diffraction (XRD) analysis. It was found that NaCl deposits markedly accelerated the oxidation of the AISI 1020 steel. The aluminide coating on the bare steel gives the best oxidation protection by forming continuous alumina scale (Al<sub>2</sub>O<sub>3</sub>). The degradation of aluminide layer and alumina scale on the steel are associated by chloridation/oxidation cyclic reactions. In addition, the released chlorine will be as catalytic actions and leads to the formation of loose Al<sub>2</sub>O<sub>3</sub> during corrosion.

### Introduction

Commercial AISI 1020 steel can be considered as a candidate material for the use of pipelines system in the Geothermal Power Plant in Ulubelu, Lampung-Indonesia. It is well known that the presence of corrosive gas either chlorine or sulfur in the steam atmosphere, noticeably increases the rates of corrosion of the steel pipe component. Previous studies indicate that the chlorine in the atmosphere contributes greatly to high-temperatures corrosion [1–3]. One method of increasing the steel's resistance to chlorine attack is the hot-dip aluminizing. This method is both cheaper and more simple than other coating methods [4]. The aluminide layer formed on the steel can form the protective alumina layer (Al<sub>2</sub>O<sub>3</sub>) that it later protects the steel from severe oxidation attack during application for the electrical power plant [5]. Therefore, both production and maintenance cost for the steam pipelines system can be reduced and thus the electrical energy production is cheaper to being soon generated for people, industry, etc.

This study focused on the oxidation of aluminized AISI 1020 steel with NaCl deposit at 700 °C for 49 h in static air. This temperature is a high temperature limit that may be experienced by the components of steel pipe. The reaction rate, morphology and corrosion product composition changes that occur on the aluminized steel were analyzed to provide insight into the mechanism of corrosion

### Experimental Procedure

The substrates were cut into 20 mm × 10 mm × 2 mm pieces from commercial AISI 1020 steel. The details of the specimen preparation and aluminizing process in the molten Al with a little Si bath at 700 °C for 16 s were similar to a previous study [5].

NaCl deposit was obtained by spraying 20 wt.% NaCl solution on the both of largest surface specimen placed on hot plate at 200 °C for 10 s. After NaCl deposition, the specimen was weighed and put into a mini crucible with size 5 mL and then exposed in the box furnace at 700 °C for a various time 1–49 h. Plot of the curve of weight gain versus oxidation time (h) is obtained to predict the oxidation resistance of bare steel and aluminized steel at 700 °C. Only the morphology, microstructure and chemical composition of the aluminized specimens are observed using Scanning Electron Microscopy (SEM) and Electron Dispersive Spectroscopy (EDS). Phases formed were examined by X-ray Diffraction (XRD).

## Results and Discussion

**Oxidation Kinetics.** Fig. 1a shows the high-temperature corrosion kinetics of both bare and aluminized steel at 700 °C. The bare steel not only had the highest weight gain, but also had been attacked severely by chlorine corrosion after 49 h. The weight gain of bare steel and aluminized steel with NaCl deposit is increased by factor of 1.5 and 16, respectively. For 49 h test, the weight gain of the aluminized steel exhibits the best corrosion resistance.

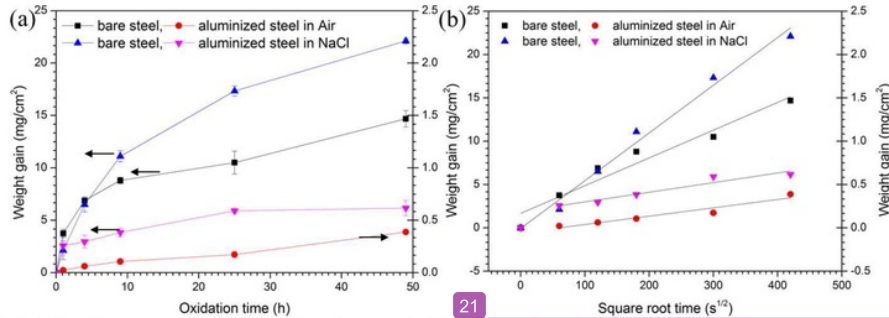


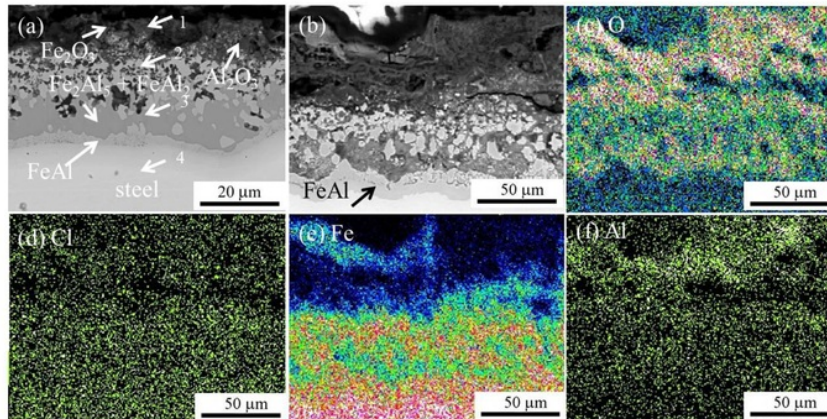
Figure 1. (a) Isothermal oxidation kinetics and (b) plots of weight gain per unit area vs. square root time for bare and aluminized AISI 1020 steel at 700 °C

The kinetics data  $(W/A_0) = k_p t^n$ , is plotted in Fig. 1b. According to the near regression calculation from Fig. 1b, the kinetics rate for the bare steel is  $1.0256 \times 10^{-9} \text{ g}^2 \text{ cm}^{-4} \text{ s}^{-1}$  and for the aluminized steel is  $9.274 \times 10^{-13} \text{ g}^2 \text{ cm}^{-4} \text{ s}^{-1}$  in air oxidation. Whereas, the kinetics rate of bare and aluminized steel with NaCl deposit is  $3.034 \times 10^{-9} \text{ g}^2 \text{ cm}^{-4} \text{ s}^{-1}$  and  $1.236 \times 10^{-10} \text{ g}^2 \text{ cm}^{-4} \text{ s}^{-1}$ , respectively. There was a substantial weight gain difference for the bare and the aluminized steel with/without NaCl deposit oxidized in static air for 49 h. The aluminide layer formed on the steel substrate gives best performance during high-temperature oxidation by forming the protective  $\text{Al}_2\text{O}_3$  layer. However, the presence of chlorine leads to a fast corrosion rate and the degradation of alumina ( $\text{Al}_2\text{O}_3$ ) layer fails to protect the steel substrate against oxidant gas which contains chlorine because of continuously outward diffusion of Al to form  $\text{Al}_2\text{O}_3$  and aluminum chlorides. Therefore, supply Al-atoms from the aluminide layer is decreased to a lower concentration and Fe-atoms can diffuse out of iron rich areas to the further reaction in the formation of iron oxide nodules.

**Microstructures and Corrosion Mechanisms.** Aluminum top-coat and intermetallic layer consisting of  $\text{Fe}_2\text{Al}_5$  and  $\text{FeAl}_3$  on the steel substrate are the typical phases constitution after hot-dip in either pure-Al or Al with a little Si [4,5]. The experimental temperature (700 °C) in this study was similar to a previous research and the phase constitution of the aluminized layers in our the aluminized AISI 1020 steel oxidized in static air for 1–9 h exposure, has been reported [5]. After oxidation in air for short-time exposure,  $\text{Fe}_2\text{Al}_5$  and  $\text{FeAl}_2$  were mainly formed in the aluminide layer at 700 °C, while  $\text{FeAl}$  were formed on the steel substrate [4–6]. Although the testing temperature in this study is lower than the melting point of NaCl (801 °C) [7]. According to Fig. 1b, the corrosion rate of aluminized steel is at least three orders of magnitude higher than that of air oxidation. Fig. 2a and 2b, respectively show the typical cross-sectional micrographs of aluminized steel after hot corrosion for 25 h and 49 h, indicating that NaCl induces hot corrosion of alloy and results in the formation of uniform attack in the aluminide layer.

SEM observation and EDS elements analysis of the aluminized specimen oxidized for 25 h (Fig. 2a) shows that the concentration of Cl (0.06 wt%) at the point 4 is lower than those of the point 2 (0.21 wt%) and 3 (0.13 wt%). The highest concentration of Cl (0.56 wt%) is detected at the point 1. The EDS elements mapping examination of aluminized specimen corroded for 49 h (Fig. 2b) reveals that the outermost region of the external scale is rich in both iron and aluminum oxides (Fig. 2c), while some chlorides can be observed in the aluminide layer (Fig. 2d). Iron is relatively much

more detected in outermost region (Fig. 2e), while aluminum is nearly depleted in the external scale due to the formation of the volatile aluminum chlorides ( $\text{AlCl}_3$ ) and inward diffusion into the steel substrate.



27

Figure 2. Cross-sectional SEM images of aluminized steel after oxidation (a) for 25 h, (b) 49 h at 700 °C, and (c–f) EDS map of elements O, Cl, Fe and Al on the cross sectional Fig. 2b

A different surface morphologies of aluminized steel after air oxidation and hot corrosion is shown in Fig. 3. For 4 h-air oxidation, the  $\text{Fe}_2\text{Al}_5$  phase with a thin  $\text{Al}_2\text{O}_3$  at the outerlayer can be observed using SEM and EDS examination (Fig. 3a). For a longer-oxidation (49 h), at the outer layer of the aluminide layer, only  $\text{Al}_2\text{O}_3$  scale is detected by XRD and SEDM/EDS examinations, no iron oxide is found at outer layer (Fig 3b). It shows that the alumina scale gives the best protection of the AISI 1020 steel in air oxidation for 49 h.

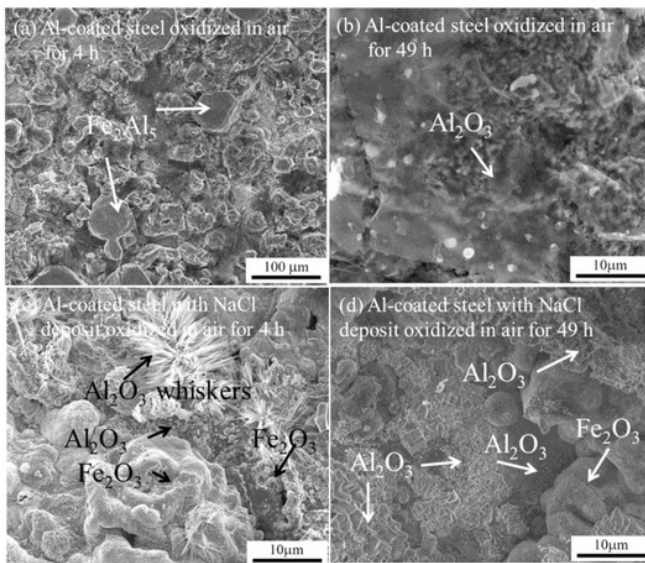


Figure 3. SEM Surface morphologies of aluminized AISI 1020 steel with/without NaCl deposit after oxidation test

Many studies [1–3] have reported the hot corrosion induced by NaCl deposits on Fe–Al base alloys that chlorine is the primary corrosive species, which accelerates the corrosion rate by forming volatile metallic chlorides. The increase in weight gain and the deposits of corrosion product on the surface of specimen during corrosion indicate that large amounts of Al-rich oxides and Fe-rich oxides are formed during corrosion. These oxides could be formed by a direct reaction between

metal and oxygen and however should be considered. Fig. 3c shows the top view of scales formed after the 4-hr oxidation at 700 °C, implying that the scale is not protective and thus the corrosion rate in this stage becomes faster. XRD and EDS analysis reveal that the corrosion scale consists of mainly  $\text{Al}_2\text{O}_3$ , and  $\text{Fe}_2\text{O}_3$  and a small amount of  $\text{FeCl}_2$ . Aluminium chloride ( $\text{AlCl}_3$ ) is not detected. In this study,  $\text{Al}_2\text{O}_3$  whiskers and  $\text{Fe}_2\text{O}_3$  grew on areas containing higher amounts of chlorine, such as cracks and voids of the surfaces of  $\text{Al}_2\text{O}_3$  and  $\text{Fe}_2\text{O}_3$  scales (Fig. 3c).

The Al-oxide whiskers' growth implied that chlorine from  $\text{NaCl}_{(s)}$  was present in the oxidizing atmosphere performing a catalyst role to increase the oxidation rate of the oxides in one direction. The growth of the  $\text{Al}_2\text{O}_3$  whiskers is attributed to the vaporization of low melting point of  $\text{AlCl}_3$  ( $182\text{ }^\circ\text{C}$ ) and high vapor pressure of the  $\text{AlCl}_3$  [7], produced during the chloridation process of the aluminide layer:  $2\text{Al} + 3\text{Cl}_{2(g)} = 2\text{AlCl}_{3(g)}$  ( $\Delta G_{700} = -471.6\text{ kJ}$ ). In addition, the  $\text{Fe}_2\text{O}_3$  scale grows because a vacancies defects of  $\text{Al}_2\text{O}_3$  can provide a rapid diffusion tunnel of oxygen for formation of  $\text{Fe}_2\text{O}_3$  scale [4,8]. Since the high vapor pressure of  $\text{AlCl}_3$  forced  $\text{AlCl}_3$  to volatilize outward through voids or cracks in the  $\text{Fe}_2\text{Al}_5 + \text{FeAl}_2$  layer a high partial pressure of oxygen environment, causing whisker growth  $\text{Al}_2\text{O}_3$  by reaction:  $4\text{AlCl}_{3(g)} + 3\text{O}_{2(g)} = 2\text{Al}_2\text{O}_{3(s)} + 6\text{Cl}_{2(g)}$  ( $\Delta G_{700} = -592.4\text{ kJ}$ ). Meanwhile, oxygen in the atmosphere can penetrate through the interconnected voids and cracks into the aluminide layer and leads to the  $\text{Al}_2\text{O}_3$  whisker being gradually replaced by the uniform growing  $\text{Al}_2\text{O}_3$  scale (Fig. 3d) due to the fact that the driving force for oxidation is higher than that for chloridation [8]. Similarly, the chloridation/oxidation reaction of  $\text{Fe}_2\text{O}_3$  formation, is  $2\text{Fe} + 3\text{Cl}_{2(g)} = 2\text{FeCl}_{3(g)}$  ( $\Delta G_{700} = -157.5\text{ kJ}$ ), and the followed by evaporation of volatile  $\text{FeCl}_3$ . The  $\text{FeCl}_{3(g)}$  is converted into iron oxide by reaction:  $4\text{FeCl}_{3(g)} + 3\text{O}_{2(g)} = 2\text{Fe}_2\text{O}_3 + 6\text{Cl}_{2(g)}$  ( $\Delta G_{700} = -109.3\text{ kJ}$ ). In addition, some chlorine is generated by both the oxidation of  $\text{AlCl}_3$  and  $\text{FeCl}_3$  can penetrate back into the aluminide layer to trigger oxidation/chloridation cyclic reactions and later destroys the aluminide layer after long-term oxidation (see in Fig. 2b). Fe-rich oxide nodules grow with the  $\text{Al}_2\text{O}_3$  scale and thus the protective  $\text{Al}_2\text{O}_3$  layer fails to protect the steel. Therefore, the weight gain of specimen is increased (Fig. 1a).

### Summary

The presence of  $\text{NaCl}$  in deposits inhibits the formation of protective oxide scale, leading to the acceleration of hot corrosion of aluminized Al 1020 steel. Corrosion products are found to be  $\text{Al}_2\text{O}_3$ ,  $\text{Fe}_2\text{O}_3$  nodules, and  $\text{FeCl}_2$ . The depletion of aluminum in the aluminide layer is caused by the evaporation of  $\text{AlCl}_3$ , and continuously increases the corrosion rate and the degradation of the aluminide layer. A rapid Fe-oxide nodules' growth and a amount of aluminum oxide formation significantly result an increase in weight gain of the aluminized specimen.

### Acknowledgement.

This research was financially supported by the Ministry of Research and Technology-Republic of Indonesia via the National Inovation System under contract No: 66/SEK/INSINAS/PPK/I/2013.

### References

- [1] C.J. Wang, J.W. Lee and T.H. Twu: Surf. Coat. Technol. Vol. 163–164 (2003), p. 37
- [2] C.J. Wang and C.C. Li Surf. Coat. Technol. Vol. 177–178 (2004), p. 37
- [3] G. Han and W.D. Cho: Oxid. Metals Vol. 58(3/4) (2002), p. 439
- [4] C.J. Wang and M. Badaruddin: Surf. Coat. Technol. Vol. 205 (2010), p. 1200
- [5] M. Badaruddin, Suharno and A.W. Hanif: The Proceeding of National Seminar of Mechanical Engineering XI, October 16–17, Yogyakarta Vol. 1(1) (2012), p. 1439
- [6] M. Badaruddin and C.J. Wang: Advanced Materials Research Vol. 79-82 (2009), p. 1775
- [7] J.G. Speight: Lange's Handbook of Chemistry, 16<sup>th</sup>Ed. Mc Graw-Hill, (2002), p. 18.
- [8] H.H. Liu, W.J. Cheng and C.J. Wang: Appl. Surf. Sci. Vol. 257 (2011), p. 10645

18

**Advances in Materials, Processing and Manufacturing**

[10.4028/www.scientific.net/AMR.789](http://10.4028/www.scientific.net/AMR.789)

**Hot Corrosion of Aluminized 1020 Steel with NaCl Deposit**

[10.4028/www.scientific.net/AMR.789.463](http://10.4028/www.scientific.net/AMR.789.463)

# Hot Corrosion of Aluminized 1020 Steel with NaCl Deposit

---

## ORIGINALITY REPORT

---

**42%**

SIMILARITY INDEX

**15%**

INTERNET SOURCES

**40%**

PUBLICATIONS

**9%**

STUDENT PAPERS

---

## PRIMARY SOURCES

---

- 1** Hsiao-Hung Liu, Wei-Jen Cheng, Chaur-Jeng Wang. "The mechanism of oxide whisker growth and hot corrosion of hot-dipped Al–Si coated 430 stainless steels in air–NaCl(g) atmosphere", *Applied Surface Science*, 2011 **7%**  
Publication

---
- 2** Muhammad Ali Abro, Dong Bok Lee. "High Temperature Corrosion of Al Hot-Dipped Low Carbon Steels in N<sub>2</sub>/H<sub>2</sub>S-Mixed Gases", *Defect and Diffusion Forum*, 2016 **6%**  
Publication

---
- 3** Charng-Cheng Tsaur, James C. Rock, Chaur-Jeng Wang, Yung-Hua Su. "The hot corrosion of 310 stainless steel with pre-coated NaCl/Na<sub>2</sub>SO<sub>4</sub> mixtures at 750°C", *Materials Chemistry and Physics*, 2005 **3%**  
Publication

---
- 4** Mohammad Badaruddin, Chaur Jeng Wang, Yudhistyra Saputra, Abu Khalid Rivai. "High Temperature Corrosion of Aluminized AISI 4130 **2%**

# Steel with the Different Composition of NaCl/Na<sub>2</sub>SO<sub>4</sub> Deposits", Makara Journal of Technology, 2015

Publication

5

Wang, C.J.. "The dependence of high temperature resistance of aluminized steel exposed to water-vapour oxidation", Surface & Coatings Technology, 20101125

Publication

2%

6

Chaur Jeng Wang, Mohd. Badaruddin. "The dependence of high temperature resistance of aluminized steel exposed to water-vapour oxidation", Surface and Coatings Technology, 2010

Publication

2%

7

Wang, C.J.. "Corrosion behaviors of AISI 1025 steels with electroless nickel/aluminized coatings in NaCl-induced hot corrosion", Surface & Coatings Technology, 20040130

Publication

2%

8

[zh.scientific.net](http://zh.scientific.net)

Internet Source

2%

9

[personal.its.ac.id](http://personal.its.ac.id)

Internet Source

1%

10

Badaruddin, Mohammad, Sugiyanto, and Ahmad Suudi. "Influence of Water-Vapor on the Isothermal Oxidation Behavior of Aluminized

1%



AISI 1020 Steel at Elevated Temperatures",  
Procedia Engineering, 2012.

Publication

---

11

Mohammad Badaruddin. "Na<sub>2</sub>SO<sub>4</sub> Induced Hot Corrosion of Aluminized Low Carbon Steel at 700 °C", Applied Mechanics and Materials, 2014

Publication

---

12

Badaruddin, Mohammad, Harnowo Supriadi, and Erwin. "Improvement of the High Temperature Oxidation of 1.10Cr-0.25Mo Steel at 850Â°C by Hot-dip Al Coating", Procedia Engineering, 2012.

Publication

---

13

Andika, Rachmat, and Muhammad Hikam. "Crystallographic Properties of Aluminum-Doped Barium Zirconium Titanate Thin Films by Sol Gel Process", Advanced Materials Research, 2013.

Publication

---

14

[link.springer.com](http://link.springer.com)

Internet Source

---

15

Wu, Yue, Qun Luo, Biao Zhou, Feng Jin, and Qian Li. "High-Temperature Oxidation Kinetics of Galvalume-Coated Steel Sheet", Advanced Materials Research, 2011.

Publication

---

1%

1%

1%

1%

1%

16	Submitted to University of Sheffield Student Paper	1%
17	Rosa, Eryta Septa, and Shobih Shobih. "Fabrication of Polymer Solar Cells on Flexible Substrate", Advanced Materials Research, 2013. Publication	1%
18	<a href="http://citeseerx.ist.psu.edu">citeseerx.ist.psu.edu</a> Internet Source	1%
19	Submitted to Savitribai Phule Pune University Student Paper	1%
20	Savetlana, Shirley, and Gusri Akhyar Ibrahim. "The Effect of Graphite and NBR on the Hardness of Fly-Ash/Phenolic Composite for Brake Lining Application", Materials Science Forum, 2015. Publication	1%
21	<a href="http://digitalscholarship.unlv.edu">digitalscholarship.unlv.edu</a> Internet Source	1%
22	<a href="http://www.tandfonline.com">www.tandfonline.com</a> Internet Source	1%
23	Tsaur, C.C.. "The hot corrosion of 310 stainless steel with pre-coated NaCl/Na <sup>2</sup> SO <sub>4</sub> mixtures at 750 <sup>o</sup> C", Materials Chemistry and Physics, 20050215 Publication	<1%

---

24

Submitted to University of Birmingham

Student Paper

<1%

---

25

Yao, Wen Li, Qian Li, Mou Cheng Li, Jie Yu Zhang, and Kuo Chih Chou. "Effect of Water Rinsing Temperature for Steel Substrate on Corrosion Behavior of Hot-Dip Aluminizing Coatings", *Advanced Materials Research*, 2010.

Publication

<1%

---

26

Wang, C.J.. "The high-temperature oxidation behavior of hot-dipping Al-Si coating on low carbon steel", *Surface & Coatings Technology*, 20060620

Publication

<1%

---

27

Submitted to Higher Education Commission  
Pakistan

Student Paper

<1%

---

28

Fu, G.. "Microstructural effects on the high temperature oxidation of two-phase Cu-Cr alloys in 1 atm O<sup>2</sup>", *Corrosion Science*, 200303

Publication

<1%

---

Exclude quotes

Off

Exclude matches

Off

Exclude bibliography

Off